

OPTIMIZATION OF THE HYPERTHERMIA TREATMENT OF A SKIN TUMOR CONTAINING NANOPARTICLES

MARION LARREUR^{‡,*}, BERNARD LAMIEN[†] AND HELCIO R. B. ORLANDE^{‡,*}

^{‡,*} Department of Mechanical Engineering, Politecnica/COPPE
Federal University of Rio de Janeiro, UFRJ
Cid. Universitaria, Cx. Postal: 68503, Rio de Janeiro, RJ, 21941-972, Brazil
e-mail: marion.larreur@poli.ufrj.br, helcio@mecanica.coppe.ufrj.br
web page: <http://www.mecanica.ufrj.br>

[†] Institut de Recherche Dupuy de Lôme - UMR CNRS 6027
University of Bretagne Sud
F-56100 Lorient, France
Email: lamienbernard@hotmail.com - web page: <http://www.irdl.fr>

Key words: bioheat transfer, finite volume, thermal damage, Arrhenius model, optimization

Abstract. This paper deals with the optimization of the hyperthermia treatment of skin cancer, with gold nanoshells loaded in the tumor. The physical problem involves a one-dimensional bioheat transfer problem, coupled to a radiation problem for the laser propagation within a multi-layered medium that includes several tissues. The corresponding bioheat transfer problem is governed by Pennes' equation, while the laser radiation propagation in the tissues is modelled with the diffusion δ -P1 approximation. The solution of the direct problem was obtained by finite volumes and verified with an analytic solution, as well as with the Matlab function *pdepe*. The thermal decomposition in the tissues was modelled with an Arrhenius equation, while the objective function was given by a quadratic form involving the difference between the predicted and the desired spatial variation of the thermal damage at a specific final time. Both the Levenberg-Marquardt and the Particle Swarm methods were implemented and provided similar results for the two design variables of interest in this work: the volume fraction of nanoparticles within the tumor and the laser power, by considering a fixed duration of 10 minutes for the treatment. The results obtained in this work also show that more than one treatment session is required for the total eradication of the tumor.

1 INTRODUCTION

The hyperthermia treatment of cancer has recently regained the attention of the scientific community due to developments in nanotechnology. In fact, several works can be found in the literature related to the use of nanoparticles in tumors, in order to increase the localized absorption of energy by cancerous cells and to decrease the thermal damage to surrounding healthy cells [1-6]. Different external non-intrusive energy sources have been reported for the hyperthermia treatment of cancer, like lasers in the near-infrared range, radio-frequency antennas, etc. [3,7]. Similarly, different kinds of nanoparticles have been used, such as those made of iron oxides [8]. In particular, noble metal nanoparticles can be designed in terms of their shapes and sizes to increase the plasmon resonance in a specific wavelength range, in order

to improve the energy absorption [9].

Heat transfer in tissues, induced by hyperthermia, is a complex combination of various phenomena as metabolic heat generation, blood perfusion, convection, and heat conduction, which makes it difficult to model. However, numerical simulations are necessary to provide accurate results about this process, with lower cost, time and manual work than experimental manipulations. Mathematical models describing heat transfer were developed with some approximations that limit the computational time, as the bio-heat transfer equation of Pennes [10], the P1 approximation [11], a diffusion approximation of light transport, and the Arrhenius equation for thermal damage [12].

As any cancer treatment, hyperthermia requires *a priori* planning, specific for each patient, based on the prediction of a thermal damage to the cells. Although the localized heat absorption is enhanced by the injection of nanoparticles, its efficiency needs to be improved by modifying some hyperthermia parameters to destroy cancerous cells while avoiding the damage of healthy cells [13].

The present work focuses on the optimization of the laser emissive power and the nanoparticles concentration for the hyperthermia treatment of a skin cancer, with the Levenberg-Marquardt and Particle Swarm algorithms. The subcutaneous tumor, assumed to be surrounded by healthy tissues and containing gold nanoshells, is irradiated by an external collimated laser for 10 minutes. A one-dimensional coupled radiation – bio-heat transfer equation is used to formulate the physical problem, and then solved with the finite volume method.

2 PHYSICAL PROBLEM AND MATHEMATICAL FORMULATION

In the problem examined here, the skin tissue is irradiated by an external collimated laser radiation for a duration of 10 minutes. The laser beam is perpendicular to the tissue and uniform, with a continuous and constant optical intensity, thereby the problem is considered one-dimensional. The skin is modelled as a superposition of five layers, each one homogeneous with constant thermal and optical properties, namely: epidermis, tumor (loaded with nanoparticles), papillary dermis, reticular dermis and fat.

2.1 Simple model

In order to choose the solution method for the problem detailed above, a simple model will first be studied, comparing the results of the different methods with the analytical solution. This model is a one-dimensional diffusion problem with an additional constant heat source, in a homogeneous medium with constant thermal properties. Convective boundary conditions are applied on both sides, and the initial temperature is considered constant, as it is given below:

$$\rho c_p \frac{\partial T(x, t)}{\partial t} = k \frac{\partial^2 T(x, t)}{\partial x^2} + Q \quad 0 < x < d, \quad t > 0 \quad (1.a)$$

$$-k \frac{\partial T(x, t)}{\partial x} + h_0 T(x, t) = h_0 T_\infty \quad x = 0, \quad t > 0 \quad (1.b)$$

$$k \frac{\partial T(x, t)}{\partial z} + h_d T(x, t) = h_d T_b \quad x = d, \quad t > 0 \quad (1.c)$$

$$T(x, t) = T_0 \quad 0 < x < d, \quad t = 0 \quad (1.d)$$

where ρ is the density of the tissue, c_p is the specific heat, k is the thermal conductivity, Q the heat source, h_0 and h_d the heat transfer coefficients, T_∞ and T_b the boundary temperatures, T_0 the initial temperature and d the domain length.

These equations are then solved analytically, decomposing the temperature in two terms: a homogeneous solution T_h , and a particular solution T_p :

$$T(x, t) = T_h(x, t) + T_p(x) \quad (2)$$

The particular solution is not time-dependent and can be written as a quadratic function of the position as it is given below:

$$T_p(x) = -\frac{Q}{k} \frac{x^2}{2} + Ax + B \quad (3.a)$$

$$A = \left(h_d(T_b - T_\infty) + Q d \left(1 + \frac{h_d d}{2k} \right) \right) / \left(k + h_d d + \frac{h_d k}{h_0} \right) \quad ; \quad B = T_\infty + \frac{k}{h_0} A \quad (3.b,c)$$

The homogeneous solution is obtained by separation of variables according to [14]:

$$T_h(x, t) = \sum_{m=1}^{\infty} \frac{1}{N(\beta_m)} e^{-k/\rho c_p \beta_m^2 t} X(\beta_m, x) \int_0^d (T_0 - T_p(x)) X(\beta_m, x) dx \quad (4.a)$$

$$\frac{1}{N(\beta_m)} = 2 \left[\left(\beta_m^2 + \frac{h_0^2}{k^2} \right) \left(d + \frac{h_d}{k} / \left(\beta_m^2 + \frac{h_d^2}{k^2} \right) \right) + \frac{h_0}{k} \right]^{-1} \quad (4.b)$$

$$X(\beta_m, x) = \beta_m \cos \beta_m x + \frac{h_0}{k} \sin \beta_m x \quad (4.c)$$

The β_m eigenvalues are given by the roots of the equation below:

$$\tan \beta_m d = \frac{\beta_m \left(\frac{h_0}{k} + \frac{h_d}{k} \right)}{\beta_m^2 - \frac{h_0}{k} \frac{h_d}{k}} \quad (4.d)$$

In this way, it is possible to determine the solution of the simple model and select the solution method that will be used to solve the bioheat transfer problem.

2.2 Bioheat transfer formulation

The mathematical formulation of the bio-heat transfer problem in this work is described by Pennes' model [10]:

$$\rho(x)c_p(x) \frac{\partial T(x, t)}{\partial x} = \frac{\partial}{\partial x} \left(k(x) \frac{\partial T(x, t)}{\partial x} \right) + \rho_b c_{p,b} \omega_b(x) (T_b - T(x, t)) + Q_{met}(x) + Q_{laser}(x) \quad (5.a)$$

$$0 < x < d, \quad t > 0$$

where ρ_b is the blood density, $c_{p,b}$ is the blood specific heat, ω_b is the blood perfusion rate, T_b is the blood temperature, Q_{met} is the metabolic heat source and Q_{laser} is the laser heat source, given by equation (2).

The interfaces between the different layers are assumed to be in ideal thermal contact. The temperature of the irradiated interface is considered constant and equal to T_0 , while a convective boundary condition is applied on the interface with deeper tissues, characterized by a heat

transfer coefficient h_d and a surrounding temperature T_0 . The initial temperature is considered uniform and equal to T_0 . The initial and boundary conditions are then given by:

$$T(x, t) = T_0, \quad x = 0, \quad t > 0 \quad (5.b)$$

$$k(x) \frac{\partial T(x, t)}{\partial x} + h_d T(x, t) = h_d T_0, \quad x = d, \quad t > 0 \quad (5.c)$$

$$T(x, t) = T_0, \quad 0 < x < d, \quad t = 0 \quad (5.d)$$

2.3 Laser heat source term

The laser heat source is computed from the tissue absorption coefficient K and the total fluence rate composed of a primary collimated component Φ_p and a secondary diffuse component Φ_s [5], as given by the equation below:

$$Q_{laser}(x) = K(x)[\Phi_p(x) + \Phi_s(x)] \quad (6)$$

The Beer-Lambert's law is used to determine the collimated component. It is given by:

$$\Phi_p(x) = I_{w,i} e^{-\beta_i(x-x_{w,i})} \quad (7.a)$$

where $I_{w,i}$ is the fluence rate at the irradiated surface of each layer i , β_i is the attenuation coefficient and $x_{w,i}$ is the position of the interface between layers i and $i-1$. For the first layer, we have:

$$I_{w,1} = I_0 (1 - R_{sc}) \quad (7.b)$$

with I_0 the optical intensity of the laser beam and R_{sc} the specular reflection coefficient at the external surface, which is a function of the tissue refractive index n_t :

$$R_{sc} = \left(\frac{n_t - 1}{n_t + 1} \right)^2 \quad (8)$$

The diffuse component of the total fluence rate is obtained by applying the diffusion δ -P1 approximation [11] given by:

$$\frac{d}{dx} \left(-D(x) \frac{d\Phi_s(x)}{dx} + \frac{\sigma'_s(x)g'(x)}{\beta_{tr}(x)} \Phi_p(x) \right) + K(x)\Phi_s(x) = \sigma'_s(x)\Phi_p(x), \quad 0 < x < d \quad (9.a)$$

$$-D(x) \frac{d\Phi_s(x)}{dx} + \frac{1}{2A_1} \Phi_s(x) = -\frac{\sigma'_s(x)g'(x)}{\beta_{tr}(x)} \Phi_p(x), \quad x = 0 \quad (9.b)$$

$$D(x) \frac{d\Phi_s(x)}{dx} + \frac{1}{2A_2} \Phi_s(x) = \frac{\sigma'_s(x)g'(x)}{\beta_{tr}(x)} \Phi_p(x) \quad x = d \quad (9.c)$$

with

$$D = \frac{1}{3\beta_{tr}}; \quad \beta_{tr} = K + \sigma_s(1 - g); \quad \sigma'_s = (1 - g^2)\sigma_s; \quad g' = g/(1 + g) \quad (10.a,b,c,d)$$

$$A_1 = (1 + R_f)/(1 - R_f); \quad A_2 = (1 + R_t)/(1 - R_t) \quad (10.e,f)$$

$$R_t = \omega_{tr} / [(1 + \sqrt{1 - \omega_{tr}})(1 + 2\sqrt{1 - \omega_{tr}})] \quad (10.g)$$

where g is the anisotropy factor, σ_s is the scattering coefficient, R_f is the Fresnel specular reflection coefficient, R_t is the reflection coefficient of the internal boundary and ω_{tr} is the transport albedo.

2.4 Thermal damage model

In order to optimize the hyperthermia treatment, it is first necessary to define the thermal decomposition of the irradiated tissue. The Arrhenius model is used to describe the thermal damage in this work in terms of a dimensionless damage parameter Ω [12]:

$$\Omega(x) = \int_0^t A e^{-\frac{E_a}{RT(x)}} dt \quad (11.a)$$

where A is the frequency factor, E_a is an energy barrier, R is the ideal gas constant and T is the temperature. The Arrhenius parameters A and E_a that characterize the process can be determined experimentally. Moreover, as the finite volume method will be used to solve the problem, the thermal damage will be written in the discrete form as it is given below, the index i designating the position and n the time:

$$\Omega_i^{n+1} = \Omega_i^n + A e^{-\frac{E_a}{RT_i^{n+1}}} \Delta t \quad (11.b)$$

The goals of the optimization are to maximize the destruction of the tumor and minimize the damage of the surrounding healthy cells. A target damage parameter Ω^* is thus defined with a linear evolution in time, to reach a final thermal damage of $\Omega^* = 1$ in the tumor, which corresponds to the necrosis of the tissue, and 0 in the other layers. The objective function is then written as in the equation below, considering the optimization of two parameters of the hyperthermia treatment: the optical intensity of the laser I_0 and the concentration of nanoparticles f_v .

$$\min S^*(I_0, f_v) = \int_0^{t_f} \int_0^d [\Omega(x, t, I_0, f_v) - \Omega^*(x, t)]^2 dx dt \quad (12.a)$$

The discrete form of this objective function for use with the finite volume method and optimization algorithms is written as:

$$\min S^*(I_0, f_v) = \sum_{k=1}^{IN} [\Omega_k(I_0, f_v) - \Omega_k^*]^2, \quad \Omega_k = \Omega_i^n \quad (12.b)$$

where IN is the number of finite volumes multiplied by the number of time steps

3 RESULTS AND DISCUSSIONS

3.1 Code Verification

The simple model presented by equations (1.a-d) is solved for a unidimensional medium with a thickness of 100mm and the thermal and optical properties of human fat [15]. The initial temperature is considered equal to 37°C, while the left boundary is characterized by a surrounding medium temperature $T_\infty=22.5^\circ\text{C}$ and a convective heat transfer coefficient $h_0=10\text{W}/\text{m}^2\text{K}$. For the right boundary, the convective heat transfer coefficient is $h_d=50\text{W}/\text{m}^2\text{K}$ and the temperature of the surrounding medium exchanging heat with the surface is equal to 40°C. This medium is submitted to an external constant radiation which results in a volumetric heat source rate of $100\text{W}/\text{m}^3$.

In order to compute the analytical solution of this problem, the Newton-Raphson method is used for finding the β_m eigenvalues.

Figure 1 presents the analytically computed temperature distribution after 1000s, as well as the temperatures obtained with the *pdepe* function of MATLAB, and the ones determined with the finite volume method by an explicit discretization of the equations.

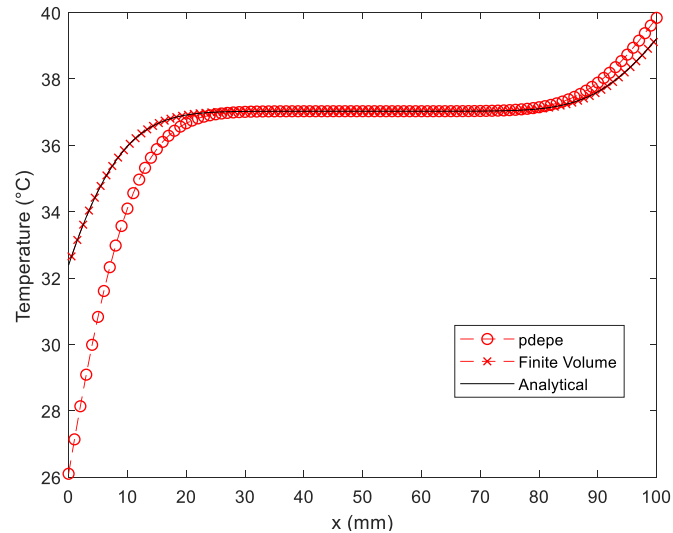


Figure 1. Temperature distribution for the simple model at $t=1000s$

The results obtained with the finite volume method perfectly agree with the analytical solution at the graph scale. However, the *pdepe* function, a MATLAB solver for partial differential equations, computes a temperature distribution quite different from the analytical one, especially near the convective boundaries.

As the Pennes' bioheat transfer equation is more complex than the model used for the verification, the finite volume method, which is more accurate than the *pdepe* function, will be used to simulate the temperature and thermal damage for the hyperthermia treatment.

3.2 Temperature and thermal damage modelling for the skin cancer

The geometry of the skin considered in this work is divided in five layers with a total thickness of 3.6mm, as represented by Figure 2. The initial temperature is considered equal to 37°C , which is also the blood temperature, T_b . The temperature of the irradiated boundary is constant and equal to T_0 , while the right boundary presents a convective heat transfer coefficient $h_d=50\text{W}/\text{m}^2\text{K}$ [2].

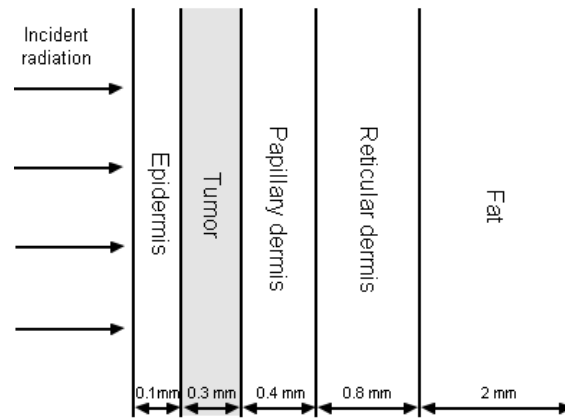


Figure 2: Unidimensional skin representation

The blood density and specific heat are respectively equal to 1060 kg/m^3 and 3770 J/kgK , while the thermal and optical properties of the other tissues are listed in Table 1 [15-17].

Table 1: Tissue properties [15-17]

	Epidermis	Tumor	Papillary dermis	Reticular Dermis	Fat
$\rho \text{ (kg/m}^3\text{)}$	1200	1030	1200	1200	1000
$c_p \text{ (J / kg K)}$	3589	3582	3300	3300	3674
$k \text{ (W / m K)}$	0.235	0.558	0.445	0.445	0.185
$Q_{met} \text{ (W/m}^2\text{)}$	0	3680	368.1	368.1	368.4
$\omega_b \text{ (s}^{-1}\text{)}$	0	0.0063	0.0002	0.0013	0.0001
$K \text{ (m}^{-1}\text{)}$	800	50	15	15	2.6
$\sigma_s \text{ (m}^{-1}\text{)}$	17500	6000	17500	17500	12000

The first and second layers, which correspond to the epidermis and the tumor, respectively, are supposed to contain gold nanoshells, thus increasing their absorption of the laser radiation. The absorption and scattering coefficients of these tissues are then obtained with the following equations [2]:

$$K' = K + 0.75f_v \frac{Q_a}{a} \quad (13.a)$$

$$\sigma_s' = \sigma_s + 0.75f_v \frac{Q_s}{a} \quad (13.b)$$

where $Q_a=7.828$ and $Q_r=1.144$ are efficiency factors, a is the radius of the nanoparticles assumed equal to 20 nm and f_v is the volumetric fraction of nanoparticles, assumed here as 2×10^{-6} [2].

The skin, which presents a refractive index $n_t = 1.4$ and an anisotropy factor $g = 0.9$, is irradiated from the left by a laser with a constant optical intensity of 20 kW/m^2 [2]. The diffuse component of the fluence rate is determined using the method of successive over-relaxation for solving the δ -P1 approximation, assuming the coefficient A_1 equal to zero.

The finite volume method with explicit scheme is then implemented and used to obtain the results presented in the figure 2, showing the effects of the nanoparticles injection on the temperature distribution (figure 2a) and fluence rate and volumetric heat source (figure 2b).

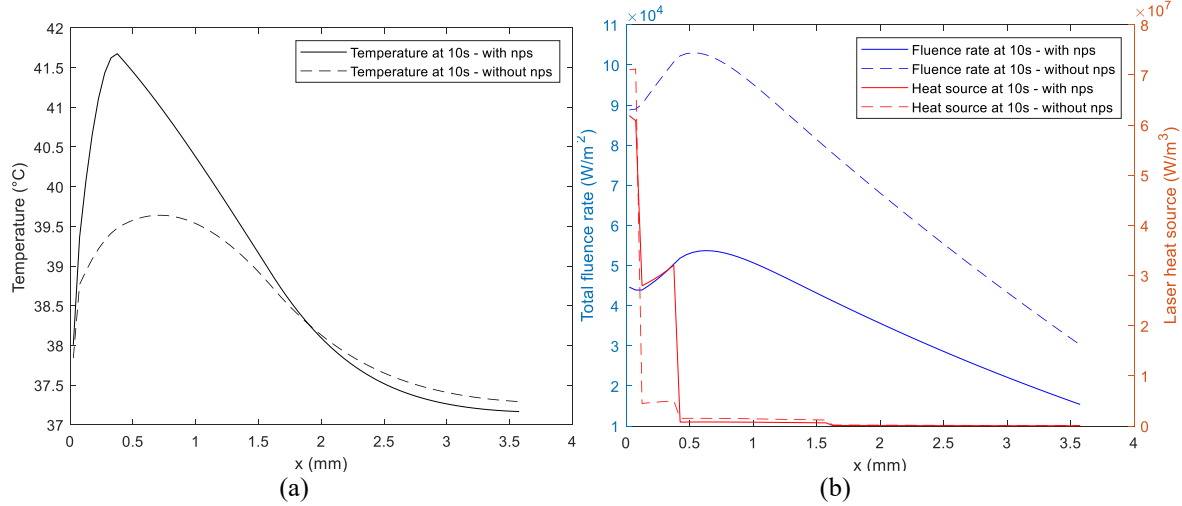


Figure 2: Effects of the nanoparticles injection at 10s on (a) the skin temperature and (b) the total fluence rate and the laser volumetric heat source

As can be seen in Figure 2a, the temperature distribution presents a peak at 41.7°C after 10s in the tumor region, between 0.3 and 0.4 mm, with the tissue embedded with gold nanoshells. For the tissue without nanoparticles, the maximum temperature is reached in the papillary dermis, which increases the risk of damaging healthy cells rather than cancerous cells. Figure 2b highlights the radiation absorption in the skin containing nanoparticles, where a strong attenuation of the total fluence rate is observed, as well as a higher volumetric heat source in the tumor.

For the thermal damage modelling, Arrhenius parameters are taken from the experimental results of [18] for the belly skin, where the activation energy E_a is considered equal to 3.935×10^5 J/mol and the frequency factor A has the value of 1.151×10^{61} s⁻¹. Equation (11.b) is then applied to compute the thermal damage parameter from the temperature obtained with the finite volume method, assuming the initial thermal damage equal to zero.

Figure 3a shows the values of the thermal damage parameter in the different layers. We notice that the thermal damage follows the evolution of the temperature presented by figure 2a, with a peak at the end of the tumor region and a strong attenuation in the dermis and fat. It can be observed in figure 3b that the thermal damage increases over time, which corresponds to the Arrhenius model. However, the maximum value is only 4.4×10^{-4} after 10s, while the thermal damage parameter must reach the value of 1 to obtain the necrosis of the tumor. That is why it is necessary to apply the hyperthermia treatment on a longer duration and modify its characteristics within an optimization procedure, as described next.

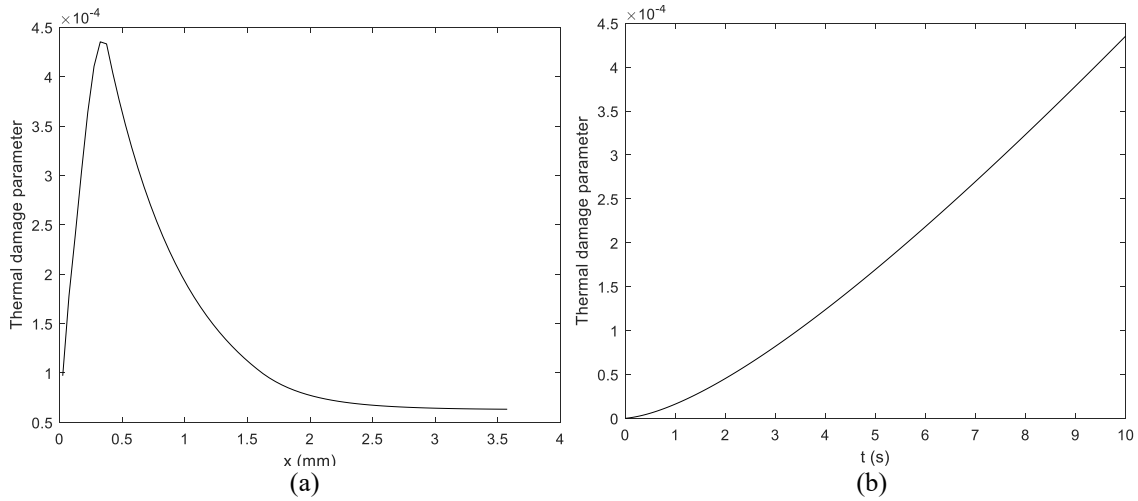


Figure 3: Evolution of the thermal damage parameter in the skin (a) as a function of the position ($t=10$ s) (b) as a function of time ($x=0.375$ mm, tumor)

3.3 Optimization of the thermal damage

For the optimization of the hyperthermia treatment, the final time is fixed and equal to 10 minutes, while two parameters are modified to find the minimum of the objective function: the laser optical intensity I_0 and the nanoparticles volumetric fraction f_v . The optical and thermal properties of the different layers of the skin, the Arrhenius constants and the laser and nanoparticles characteristics remain the same as for the example in the previous section.

The thermal damage computed with equation (11.b) is compared with the ideal one through the objective function. The ideal thermal damage parameter is considered to follow a linear evolution in time starting from 0 to reach 1 in the tumor and stay at 0 in the healthy cells. A shape parameter has been added to this ideal thermal damage function to smooth the distribution in the boundaries of the tumor so that it is more similar to the real one.

Two different optimization algorithms are applied to the problem, namely: the Levenberg-Marquardt method, a nonlinear least squares minimizer, and the Particle Swarm Optimization (PSO) algorithm, a population based stochastic optimization technique, implemented with a population size of 50. The table below presents the results of the algorithms obtained using an Intel Pentium 3665U @ 1.70 GHz, in a 64-bit system, with 4 Gb of RAM. Two objective functions are studied: one includes the thermal damage for all time steps during the treatment, while the other consider only the thermal damage at the final time, that is, 10 minutes, which correspond to the maximum value of the thermal damage since it increases in time.

Table 2: Results of the optimization algorithms

Algorithm	Objective Function	Computational Time	Stopping Criteria	f_v	I_0 (W/m ²)
Levenberg-Marquardt	All time	28533 s	Step size 10^{-30}	8.08×10^{-5}	66116
	Final time	3838 s	Step size 10^{-50}	8.48×10^{-5}	66328
Particle Swarm	All time	98782 s	50 iterations	8.23×10^{-5}	66572
	Final time	128199 s	100 iterations	8.48×10^{-5}	66328

As can be seen in Table 2, the two algorithms give identical results for the optimization of the objective function at final time, with a higher computational time for the implemented PSO method. The stopping criteria for the all-time evaluation of the objective function are considered lower than for the final time evaluation, due to a higher computational time: the step size tolerance is 10^{-30} instead of 10^{-50} for the Levenberg-Marquardt algorithm, and the maximal number of iterations is 50 instead of 100 for the PSO. For this reason and the possible deviations of the real and ideal thermal damages in time, the resulting parameters are slightly different from the ones of the final thermal damage optimizations. By any way, the optimized values f_v of I_0 and are consistent for all cases considered.

Figure 4 presents the temperature and thermal damage distributions computed with $f_v = 8.48 \times 10^{-5}$ and $I_0 = 66328$ W/m², the parameters resulting from the final thermal damage optimization.

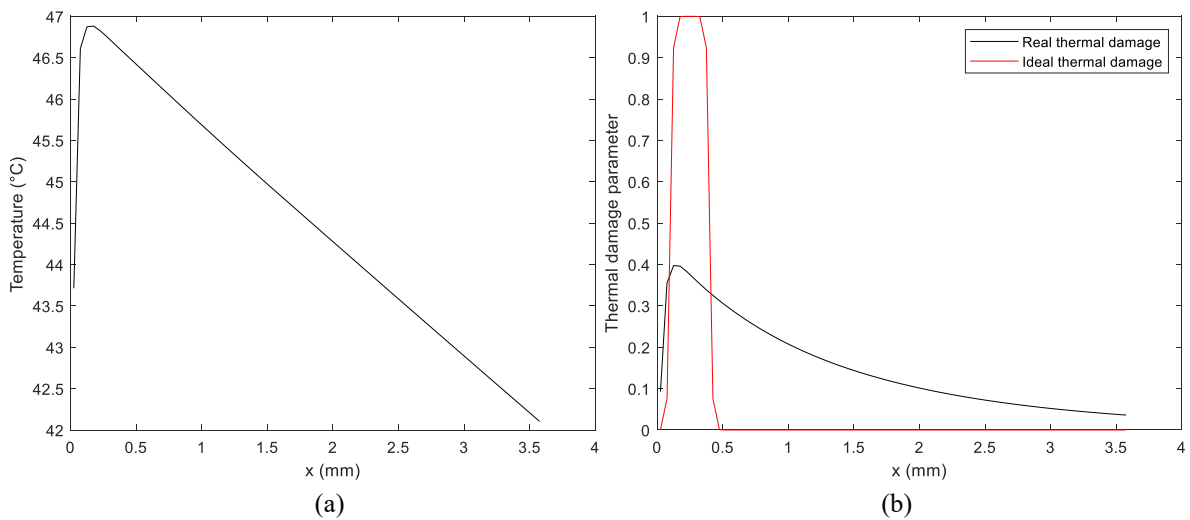


Figure 4: Distribution after 10min of the optimized hyperthermia treatment on the skin of: (a) temperature (b) thermal damage

The temperature presents a peak of 46.8°C in the tumor region, around 0.2mm, where the thermal damage parameter reaches a maximum value of 0.4, next to the left boundary of the tumor.

However, the optimized thermal damage is still lower than the ideal one after 10 minutes of exposure and the cancerous tissue is not fully destroyed with one single session of the hyperthermia treatment. A second session is therefore needed to increase the thermal damage in the tumor, while maintaining reasonable temperatures. For this second session, the skin was assumed to cool down and return to T_0 between the two applications. The hyperthermia treatment is then applied with the same optimal conditions for 10 minutes, with the initial thermal damage of the second session considered equal to the final thermal damage of the first session. As can be seen in Figure 5, a second session of the hyperthermia treatment with the same optimal parameters of the first session doubles the thermal damage of the skin, with a peak at 0.8, which still remains in the tumor region.

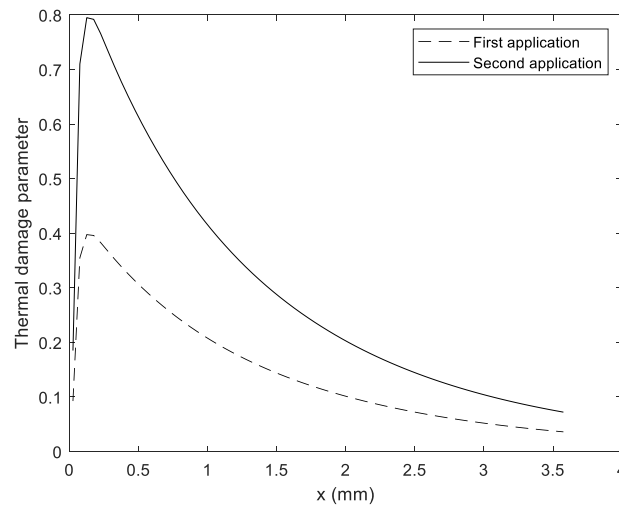


Figure 5: Thermal damage distribution in the skin after a second application of the 10min hyperthermia treatment

4 CONCLUSIONS

From this simulation, it can be concluded that the Levenberg-Marquardt and PSO algorithms can be used for the optimization of the hyperthermia treatment. It was also shown that, with a fixed exposure duration of 10 minutes, at least a second session of the hyperthermia treatment is necessary to inflict a thermal damage to the tumor that approaches the tissue necrosis. On the other hand, the optimization of parameters like the beam size, the time of exposure or a non-constant laser emissive power may also be relevant to provide a more suitable treatment.

ACKNOWLEDGEMENTS

The authors are thankful for the support provided by CNPq, CAPES (Finance Code 001) and FAPERJ, Brazilian agencies for the fostering of science.

REFERENCES

- [1] O’Neal D.P., Hirsch L.R., Halas N.J. et al. 2004 Photo-thermal tumor ablation in mice using near infrared-absorbing nanoparticles *Cancer Letters* **209**(2):171-6
- [2] Dombrovsky L.A., Timchenko V., Jackson M. and Yeoh G.H. 2011 A Combined Transient Thermal Model for Laser Hyperthermia of Tumors with Embedded Gold Nanoshells *Int. J. Heat Mass Transf.* **54**:5459–69
- [3] Bruno A.b., Maurente A., Lamien B. and Orlande H.R.B. 2016 Numerical simulation of nanoparticles assisted laser photothermal therapy: a comparison of the P-approximation and discrete ordinate methods *J Braz. Soc. Mech. Sci. Eng.* **39**:621-630
- [4] Kurgan E and Gas P 2011 Treatment of Tumors Located in the Human Thigh using RF Hyperthermia *Prz. Elektrotechniczny* **87**:103–6
- [5] Lamien B., Orlande H.R.B., Elicabe G.E. and Maurente A.J. 2014 State Estimation Problem in Hyperthermia Treatment of Tumors Loaded with Nanoparticles *Proceedings of the 15th International Heat Transfer Conference, IHTC-15* (Kyoto, Japan) pp 1–15
- [6] Bermeo Varon L.A., Orlande H.R.B. and Elicabe G.E. 2015 Combined Parameter and State Estimation in the Radiofrequency Hyperthermia Treatment of Cancer *Heat Transf. Part A Apl.* **accept**:1–31
- [7] Wu L., McGough R.J., Ali Arabe O. and Samulski T.V. 2006 An RF phased array applicator designed for hyperthermia breast cancer treatments *Phys. Med. Biol.* **51**:1-20
- [8] Yadel C., Michel A., Casale S. and Fresnais J. 2018 Hyperthermia Efficiency of Magnetic Nanoparticles in Dense Aggregates of Cerium Oxide/Iron Oxide Nanoparticles *Appl. Sci.* **8**, 1241
- [9] Tuersun P., Han X. 2014 Optimal dimensions of gold nanoshells for light backscattering and absorption based applications. *J Quant Spectrosc Radiat Transf* **146**:468–474
- [10] Pennes H.H. 1948 Analysis of tissue and arterial blood temperature in the resting human forearm *J Appl Physiol* **1**(2):93–122
- [11] Star W.M. 2011 “Diffusion Theory of Light Transport”. In Welch, A. J., Van Gemert, J.C.M. Eds, *Optical-Thermal Response of Laser irradiated Tissue*, 2 ed., Dordrecht Heidelberg London New York, Springer
- [12] Pearce J.A. 2010 Models for Thermal Damage in Tissues: Processes and Applications *Critical Reviews in Biomedical Engineering* **38**(1):1-20
- [13] Feng Y., Fuentes D., Hawkins A. et al. 2009 Nanoshell-mediated laser surgery simulation for prostate cancer treatment *Eng. Comput.* **25**(1):3-13
- [14] Ozisik, M.N. 1985 ”Transfer A Basic Approach” MacGraw-Hill Book Company.
- [15] Çetingül, M. P., Herman, C. 2010 A Heat transfer model of skin tissue for the detection of lesions: sensitivity analysis *Physics in Medicine and Biology* **55**:5933-5951
- [16] Çetingül, M. P., Herman, C. 2011 Quantification of the thermal signature of a melanoma lesion *Int. J. Therm. Sci.*, **50**: 421-431
- [17] Tuchin V. 2000 *Tissue Optics, Light Scattering Methods and Instruments for Medical Diagnosis*, Washington: SPIE
- [18] Xu F., Seffen K.A., Lu T.J. 2008 Temperature-Dependent Mechanical Behaviors of Skin Tissue *Int. J. Comp. Sci.* **35**:1-13